

Inclusive studies of two- and three-nucleon short-range correlations in ^3H and ^3He

S. Li,^{1,2,*} S. N. Santiesteban,¹ J. Arrington,^{2,3} R. Cruz-Torres,⁴ L. Kurbany,¹ D. Abrams,⁵
 S. Alsalmi,^{6,7} D. Androic,⁸ K. Aniol,⁹ T. Averett,¹⁰ C. Ayerbe Gayoso,¹⁰ J. Bane,¹¹
 S. Barcus,¹⁰ J. Barrow,¹¹ A. Beck,⁴ V. Bellini,¹² H. Bhatt,¹³ D. Bhetuwal,¹³ D. Biswas,¹⁴
 D. Bulumulla,¹⁵ A. Camsonne,¹⁶ J. Castellanos,¹⁷ J. Chen,¹⁰ J-P. Chen,¹⁶ D. Chrisman,¹⁸
 M. E. Christy,^{14,16} C. Clarke,¹⁹ S. Covrig,¹⁶ K. Craycraft,¹¹ D. Day,⁵ D. Dutta,¹³
 E. Fuchey,²⁰ C. Gal,⁵ F. Garibaldi,²¹ T. N. Gautam,¹⁴ T. Gogami,²² J. Gomez,¹⁶
 P. Guèye,^{14,18} A. Habarakada,¹⁴ T. J. Hague,⁶ J. O. Hansen,¹⁶ F. Hauenstein,¹⁵
 W. Henry,²³ D. W. Higinbotham,¹⁶ R. J. Holt,^{24,3} C. Hyde,¹⁵ K. Itabashi,²² M. Kaneta,²²
 A. Karki,¹³ A. T. Katramatou,⁶ C. E. Keppel,¹⁶ M. Khachatryan,¹⁵ V. Khachatryan,¹⁹
 P. M. King,²⁵ I. Korover,²⁶ T. Kutz,¹⁹ N. Lashley-Colthirst,¹⁴ W. B. Li,¹⁰ H. Liu,²⁷
 N. Liyanage,⁵ E. Long,¹ J. Mammei,²⁸ P. Markowitz,¹⁷ R. E. McClellan,¹⁶
 F. Meddi,²¹ D. Meekins,¹⁶ S. Mey-Tal Beck,⁴ R. Michaels,¹⁶ M. Mihovilović,^{29,30,31}
 A. Moyer,³² S. Nagao,²² V. Nelyubin,⁵ D. Nguyen,⁵ M. Nycz,⁶ M. Olson,³³ L. Ou,⁴
 V. Owen,¹⁰ C. Palatchi,⁵ B. Pandey,^{14,†} A. Papadopoulou,⁴ S. Park,¹⁹ S. Paul,^{34,‡}
 T. Petkovic,⁸ R. Pomatsalyuk,³⁵ S. Premathilake,⁵ V. Punjabi,³⁶ R. D. Ransome,³⁷
 P. E. Reimer,³ J. Reinhold,¹⁷ S. Riordan,³ J. Roche,²⁵ V. M. Rodriguez,³⁸ A. Schmidt,⁴
 B. Schmookler,⁴ E. P. Segarra,⁴ A. Shahinyan,³⁹ S. Širca,^{30,29} K. Slifer,¹ P. Solvignon,¹
 T. Su,⁶ R. Suleiman,¹⁶ H. Szumila-Vance,¹⁶ L. Tang,¹⁶ Y. Tian,⁴⁰ W. Tireman,⁴¹
 F. Tortorici,¹² Y. Toyama,²² K. Uehara,²² G. M. Urciuoli,²¹ D. Votaw,¹⁸
 J. Williamson,⁴² B. Wojtsekhowski,¹⁶ S. Wood,¹⁶ Z. H. Ye,^{43,3} J. Zhang,⁵ and X. Zheng⁵

¹*University of New Hampshire, Durham, New Hampshire 03824, USA*

²*Lawrence Berkeley National Laboratory, Berkeley, California 94720, USA*

³*Physics Division, Argonne National Laboratory, Lemont, Illinois 60439, USA*

⁴*Massachusetts Institute of Technology,
Cambridge, Massachusetts 02139, USA*

⁵*University of Virginia, Charlottesville, Virginia 22904, USA*

- ⁶*Kent State University, Kent, Ohio 44240, USA*
- ⁷*King Saud University, Riyadh 11451, Kingdom of Saudi Arabia*
- ⁸*University of Zagreb, Zagreb, Croatia*
- ⁹*California State University, Los Angeles, California 90032, USA*
- ¹⁰*The College of William and Mary,
Williamsburg, Virginia 23185, USA*
- ¹¹*University of Tennessee, Knoxville, Tennessee 37966, USA*
- ¹²*INFN Sezione di Catania, Italy*
- ¹³*Mississippi State University, Mississippi State, Mississippi 39762, USA*
- ¹⁴*Hampton University, Hampton, Virginia 23669, USA*
- ¹⁵*Old Dominion University, Norfolk, Virginia 23529, USA*
- ¹⁶*Thomas Jefferson National Accelerator Facility,
Newport News, Virginia 23606, USA*
- ¹⁷*Florida International University, Miami, Florida 33199, USA*
- ¹⁸*Michigan State University, East Lansing, Michigan 48824, USA*
- ¹⁹*Stony Brook, State University of New York, New York 11794, USA*
- ²⁰*University of Connecticut, Storrs, Connecticut 06269, USA*
- ²¹*INFN, Rome, Italy*
- ²²*Tohoku University, Sendai, Japan*
- ²³*Temple University, Philadelphia, Pennsylvania 19122, USA*
- ²⁴*California Institute of Technology, Pasadena, California 91125, USA*
- ²⁵*Ohio University, Athens, Ohio 45701, USA*
- ²⁶*Nuclear Research Center -Negev, Beer-Sheva, Israel*
- ²⁷*Columbia University, New York, New York 10027, USA*
- ²⁸*University of Manitoba, Winnipeg, MB R3T 2N2, Canada*
- ²⁹*Jožef Stefan Institute, 1000 Ljubljana, Slovenia*
- ³⁰*Faculty of Mathematics and Physics,
University of Ljubljana, 1000 Ljubljana, Slovenia*
- ³¹*Institut für Kernphysik, Johannes Gutenberg-
Universität Mainz, DE-55128 Mainz, Germany*
- ³²*Christopher Newport University, Newport News, Virginia 23606, USA*
- ³³*Saint Norbert College, De Pere, Wisconsin 54115, USA*

³⁴*William & Mary, Williamsburg, Virginia 23185, USA*

³⁵*Institute of Physics and Technology, Kharkov, Ukraine*

³⁶*Norfolk State University, Norfolk, Virginia 23529, USA*

³⁷*Rutgers University, New Brunswick, New Jersey 08854, USA*

³⁸*División de Ciencias y Tecnología, Universidad Ana G. Méndez,
Recinto de Cupey, San Juan 00926, Puerto Rico*

³⁹*Yerevan Physics Institute, Yerevan, Armenia*

⁴⁰*Syracuse University, Syracuse, New York 13244, USA*

⁴¹*Northern Michigan University, Marquette, Michigan 49855, USA*

⁴²*University of Glasgow, Glasgow, G12 8QQ Scotland, UK*

⁴³*Tsinghua University, Beijing, China*

(Dated: April 26, 2024)

Abstract

Inclusive electron scattering at carefully chosen kinematics can isolate scattering from short-range correlations (SRCs), produced through hard, short-distance interactions of nucleons in the nucleus. Because the two-nucleon (2N) SRCs arise from the same N-N interaction in all nuclei, the cross section in the SRC-dominated regime is identical up to an overall scaling factor, and the $A/{}^2\text{H}$ cross section ratio is constant in this region. This scaling behavior has been used to identify SRC dominance and to map out the contribution of SRCs for a wide range of nuclei. We examine this scaling behavior at lower momentum transfers using new data on ${}^2\text{H}$, ${}^3\text{H}$, and ${}^3\text{He}$ which show that the scaling region is larger than in heavy nuclei. Based on the improved scaling, especially for ${}^3\text{H}/{}^3\text{He}$, we examine the ratios at kinematics where three-nucleon SRCs may play an important role. The data for the largest initial nucleon momenta are consistent with isolation of scattering from 3N-SRCs, and suggest that the very-highest momentum nucleons in ${}^3\text{He}$ have a nearly isospin-independent momentum configuration, or a small enhancement of the proton distribution.

Two-nucleon short-range correlations, pairs of nucleons in nuclei with large relative but small total momenta, are generated by the strong short-range part of the nucleon-nucleon (N-N) interaction [1, 2]. Inclusive quasi-elastic scattering can isolate scattering from these high-momentum configurations in kinematics that require scattering from high-momentum nucleons [2–4]. Cleanly isolating SRCs requires large momentum transfer, Q^2 , to suppress long-range final-state interactions (FSIs) and meson-exchange currents, and also small energy transfer, ν , to suppress inelastic processes i.e. $x = Q^2/(2M\nu) > 1$, where M is the nucleon mass [2, 5].

The quasi-elastic (QE) peak at $x \approx 1$ corresponds to scattering from a low-momentum nucleon. For QE scattering at $x > 1$, any given x and Q^2 combination corresponds to a minimum initial nucleon momentum, k_{min} , for scattering to be kinematically allowed [3]. Because the mean-field contribution drops off rapidly with increasing nucleon momentum, these contributions can be excluded by going to large x and Q^2 , leaving only the contribution from 2N-SRCs. In the basic SRC model, where SRCs are assumed to be stationary (zero

* Corresponding author: ShujieLi@lbl.gov

† Current affiliation: Department of Physics & Astronomy, Virginia Military Institute, Lexington, Virginia 24450, USA

‡ Current affiliation: University of California Riverside, 900 University Ave. Riverside, CA 92521, USA

total momentum in the rest frame of the nucleus) and long-range FSIs are taken to be negligible, the high-momentum structure is generated by two-body interactions, yielding identical SRC structure at high momentum for all nuclei [1, 6]. This means that the cross sections for scattering from different nuclei in this kinematic region will be identical up to an overall scaling factor that represents the total contribution of deuteron-like SRCs in the nucleus, apart from small corrections due to the center-of-mass (CM) motion and isospin configurations of those NN pairs. As such, the cross section ratio of any nucleus A to the deuteron, σ_A/σ_{2H} should scale with respect to both x and Q^2 in this 2N-SRC region.

An examination of the $A/{}^2\text{H}$ cross section ratios with data from SLAC measurements [5] observed an A -dependent plateau in x for $x > 1.4$, independent of Q^2 for $Q^2 \geq 1.4 \text{ GeV}^2$. Later measurements mapped out the $A/{}^2\text{H}$ cross section ratio in this scaling regime, $a_2(A)$, for a variety of nuclei [7–11]. The inclusive ratios show that a_2 rises rapidly with A in light nuclei, but becomes roughly constant, $a_2 \approx 5$, for nuclei from carbon to lead [2]. They also demonstrated that the predicted scaling breaks down at low Q^2 values [4, 5, 12] due to increasing contributions from FSIs to the cross section in the numerator along with the fact that lowering Q^2 at fixed x allows scattering from lower-momentum nucleons, and thus does not isolate 2N-SRCs as cleanly. Additional measurements demonstrated that the SRCs are dominated by neutron-proton (np) pairs [11, 13–18], with pp and nn SRCs contributing only a few percent each in heavy nuclei [2], but roughly 20% in ${}^3\text{He}$ [11]. Note that while a_2 is often described as the relative number of 2N-SRC pairs in a nucleus relative to the deuteron, additional effects neglected in the basic SRC model, most notably CM motion of the SRC pair in the nucleus, yield corrections to this interpretation [2, 8, 11, 19, 20].

Going beyond 2N-SRC region, the SRC model predicts that at $x > 2$, where the 2N-SRC contributions drops rapidly, three-nucleon (3N) SRCs will dominate the cross sections such that ratios of $A/{}^3\text{He}$ may show scaling [5]. This may allow the observation and quantification of 3N-SRCs, although it is much less straightforward to predict where the 3N-SRCs should dominate [2]. In fact, 2N-SRCs will contribute to the cross section beyond $x=2$ due to CM motion of the pair, making it difficult to predict where the 2N contribution will be negligible.

While a few experiments looked for a plateau in the $A/{}^3\text{He}$ ratios at $x > 2$, there is no conclusive evidence supporting the predicted 3N-SRCs scaling [2, 21]. Previous $x > 2$ measurements at $Q^2 \approx 1.5\text{--}2 \text{ GeV}^2$ [9, 22] do not show the expected scaling behavior [23], but did not reach Q^2 values where 3N-SRC dominance is expected. Calculations from [4, 24, 25]

suggest that the data at $Q^2 \approx 3 \text{ GeV}^2$ from Ref. [8] may be sufficiently high in Q^2 to observe 3N-SRC dominance. While the data are consistent with a plateau for $x > 2.5$, they have very limited statistics and took data at only one Q^2 value. While the statistics make it difficult to claim an observation of scaling, the relative 2N-SRC and 3N-SRC contributions from [8] are observed to be consistent [24] with the prediction that the 3N-SRC probability should scale as the 2N-SRC probability squared.

While the SRC model makes clear predictions for where 2N-SRCs should dominate and provides a simple interpretation of the data, effects such as FSIs, the CM motion of SRC pairs in the nucleus, and the presence of pp and/or nn pairs in $A > 2$ nuclei can violate the assumptions of the basic SRC model presented above [2, 4]. We expect the impact of these scaling violations in the cross section to be suppressed in A_1/A_2 ratios with $A_1 \approx A_2$, e.g. ${}^3\text{He}/{}^2\text{H}$ or ${}^{48}\text{Ca}/{}^{40}\text{Ca}$ [18], where these effects will have significant cancellation between the numerator and denominator. Also, because light nuclei have smaller mean-field momenta, the mean-field cross section contributions will fall off faster and the 2N-SRC contributions, and thus the scaling behavior, should dominate at a lower values of x and Q^2 .

In this work, we examine deviations from the basic 2N-SRC model in detail and demonstrate that scaling violations are dramatically reduced in the comparison of few-body nuclei, and even more so in the comparison of the mirror nuclei ${}^3\text{H}$ and ${}^3\text{He}$. We then take advantage of the greater kinematic range of the data to study SRCs at $x > 2$, where 3N-SRCs are expected to contribute and, at some point, dominate the scattering [2, 4, 21].

Data used in this analysis were taken in Hall A at Jefferson Lab (JLab) in 2018 as part of experiments E12-11-112 and E12-14-011 [11, 26–31], along with additional ${}^3\text{He}/{}^2\text{H}$ ratios from [8]. We show cross section ratios covering the full kinematic coverage of E12-11-112, most of which has not been previously published. All of the $A/{}^2$ ratios are new results, except for the $Q^2 = 1.4 \text{ GeV}^2$ data included in Ref. [11], while ${}^3\text{H}/{}^3\text{He}$ ratios included in Ref. [26] were limited to the QE peak, $x \lesssim 1.2$.

Four identical 25 cm long aluminum cells were used to hold 70.8, 142.2, 85.0 (84.8)[32], and 53.2 mg/cm² of ${}^1\text{H}$, ${}^2\text{H}$, ${}^3\text{H}$, and ${}^3\text{He}$ (e, e') gas at room temperature [31, 33]. Electrons scattered from the target nuclei and were detected in the Hall A High Resolution Spectrometers. For each spectrometer angle, 2-4 overlapping momentum settings were used to cover an x range around the quasi-elastic (QE) peak and into the SRC region at $x > 1$. Detailed descriptions of experimental setup can be found in [34–36]. The high- Q^2 E12-11-112

E_{beam} (GeV)	θ_0 (degrees)	$\langle Q^2 \rangle$ (GeV ²)	x range	Ref.
2.222	21.778	0.6	0.6-3	[26]
2.222	23.891	0.7	0.6-2	[26]
2.222	30.001	1.0	0.7-2	[26]
4.332	17.006	1.4	0.6-3	[11]
4.325	20.881	1.9	0.9-1.7	[11]
5.766	18.000	2.6	0.5-2.1	[8]

TABLE I. Kinematics for the data included in this analysis: E_{beam} is the incoming beam energy, θ_0 is the HRS central angle, and $\langle Q^2 \rangle$ is the mean Q^2 value for the data at $x=1.5$. Note that the x range for the 0.7 GeV² deuterium data is 0.7-1.5, and that and 1.9 GeV² data set includes measurements at 17.802 degrees to extend the data down to $x = 0.7$.

data sets demonstrate clear scaling behaviors in $^3\text{H}/^2\text{H}$ and $^3\text{He}/^2\text{H}$ cross section ratios at $1.4 < x < 2$ [11]. Additional data were taken as part of E12-11-112 at lower Q^2 values, focusing on the quasielastic (QE) peak [26], with three settings extending to much larger x values as described in Table I. The extraction of the cross section ratios follows the procedures described in Ref. [11] and the kinematics of the data presented here is summarized in Table I.

We begin by examining the quality of scaling over a range of Q^2 values in the $^3\text{He}/^2\text{H}$ ratios as a function of x (top panel) and the light-cone variable α_{2N} [5] (middle panel) in Figure 1, where

$$\alpha_{2N} = 2 - \frac{q_- + 2m_N}{2m_N} \left(1 + \frac{\sqrt{W_{2N}^2 - 4m_N^2}}{W_{2N}} \right). \quad (1)$$

Here m_N is the nucleon mass, $q_- = q_0 - |\mathbf{q}|$, $W_{2N}^2 = (q + 2m_N)^2 = -Q^2 + 4q_0m_N + 4m_N^2$. The quantity α_{2N} is an approximation of the light-cone momentum fraction, α in a two-nucleon system, and is a better surrogate for initial nucleon momentum than x , as the mapping between α_{2N} and k_{min} removes Q^2 -dependent corrections in going from x to k_{min} . Because of this, the top panel of Fig. 1 shows a clear Q^2 dependence to the width of the QE peak in x which is absent when plotted against α_{2N} . For all further examinations of scaling, we will show the cross section ratios vs α_{2N} to remove these trivial kinematic scaling violations.

In the 2N-SRC region, a plateau is seen in the $^3\text{H}/^2\text{H}$ as well as $^3\text{He}/^2\text{H}$ ratios at $\alpha_{2N} > 1.2$

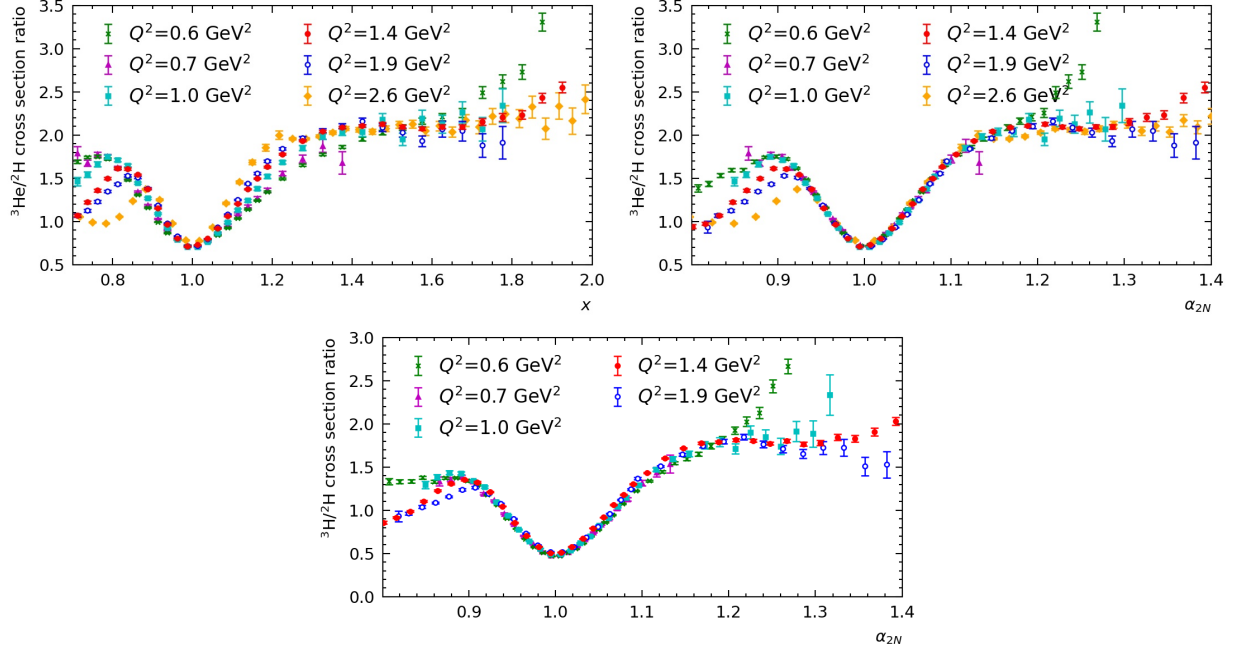


FIG. 1. ${}^3\text{He}/{}^2\text{H}$ per-nucleon cross section ratio vs x (top) and α_{2N} (middle) from this experiment and the previous high- Q^2 JLab measurement [8], along with the ${}^3\text{H}/{}^2\text{H}$ ratios vs α_{2N} (bottom). The ${}^3\text{He}/{}^2\text{H}$ (${}^3\text{H}/{}^2\text{H}$) ratios have a normalization uncertainty of 1.15% (0.8%), except for the $Q^2=2.6$ GeV^2 data [8] which has a 1.8% normalization uncertainty.

when $Q^2=1$ GeV^2 and higher. The observation of scaling behavior down to $Q^2=1$ GeV^2 is consistent with ${}^4\text{He}/{}^2\text{H}$ ratios of Ref. [5], while ${}^{56}\text{Fe}/{}^2\text{H}$ and ${}^{198}\text{Au}/{}^2\text{H}$ [5] and ${}^{12}\text{C}/{}^3\text{He}$ [12] ratios show scaling only for $Q^2 \geq 1.4$ GeV^2 . Scaling is expected at lower Q^2 values in light nuclei due to their lower mean-field momenta. On top of that, the long range FSIs are also more effectively canceled in the comparison of $A=3$ nuclei to the deuteron, which leads to scaling at even lower Q^2 and α_{2N} .

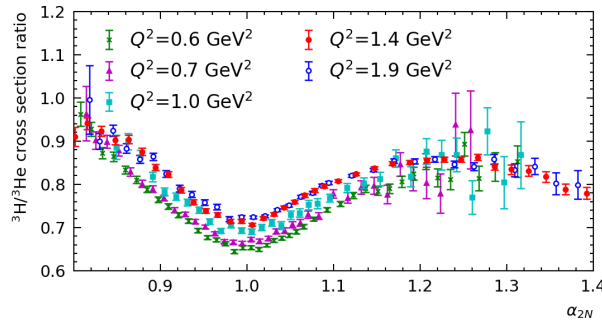


FIG. 2. ${}^3\text{H}/{}^3\text{He}$ ratios vs α_{2N} in the 2N-SRC region.

In the ${}^3\text{H}/{}^3\text{He}$ ratio, FSIs, CM motion corrections [11], and the k_{min} threshold to exclude mean field contributions should be almost identical and these scaling-violating effects should be even smaller, as shown in Figure 2. Note that the ratio at $x \approx 1$ is Q^2 -dependent because of the small difference in the Q^2 dependence of the proton and neutron quasi-elastic cross sections. This effect is normally much smaller than the difference in nuclear smearing between heavy and light nuclei, and is only obvious in the $A=3$ nuclei comparison.

Given the expanded scaling in the 2N-SRC region for ${}^3\text{He}/{}^2\text{H}$, ${}^3\text{H}/{}^2\text{H}$, and especially ${}^3\text{H}/{}^3\text{He}$ ratios, it is interesting to look at $x > 2$, i.e. beyond the deuteron elastic peak, for contributions from 3N-SRCs [2, 3]. One can make predictions for the ratios in the 3N-SRC dominant region based on simple assumptions about their momentum and isospin structure [2, 21, 27]. If the three-body system is dominated by the symmetric "triangle" configurations, where all three nucleons have similar momentum, then the probability of scattering from a high-momentum proton or neutron will reflect the number of protons and neutrons in the 3N-SRC system, yielding a result similar to the QE peak. For the kinematics of the present measurement, the ${}^3\text{H}/{}^3\text{He}$ cross section ratio would approach $(\sigma_{ep} + 2\sigma_{en})/(2\sigma_{ep} + \sigma_{en}) \approx 0.75$, where σ_{eN} are the off-shell electron-nucleon elastic scattering cross sections. The other extreme is the "linear" configuration, where the highest-momentum nucleon is balanced by two co-linear spectator nucleons, where scattering at the largest- x values will be dominated by the highest-momentum nucleon. If this is the singly-occurring nucleon, then the scattering would select the proton (neutron) in ${}^3\text{H}$ (${}^3\text{He}$), yielding $\sigma_{3H}/\sigma_{3He} \approx \sigma_{ep}/\sigma_{en} \approx 2.5$. Similarly, it would be $\sigma_{en}/\sigma_{ep} \approx 0.4$ if one of the doubly-occurring nucleons has the largest momentum. If there is no isospin preference for the highest momentum nucleon, then the measured ratio again corresponds to the number of protons and neutrons, as in the triangle configuration, giving a σ_{3H}/σ_{3He} ratio of 0.75. Thus, an increase (decrease) of the ${}^3\text{H}/{}^3\text{He}$ ratio from the 2N-SRC plateau region as 3N-SRCs begin to contribute would suggest that the 3N contribution to the ratio is larger (smaller) than the observed ratio of 0.85 in the 2N-SRC regime [11].

While these are simple limiting cases, where we assume only a single configuration contributes, an analysis of ${}^3\text{He}$ electro-disintegration suggests that the 3N-SRC is predominately formed by two consecutive 2N-SRC interactions in the linear configuration [37]. The triangle configuration can also contribute at extremely high momentum (e.g. $> 700\text{MeV}/c$), but it has significantly larger missing energy and is suppressed in inclusive scattering. The

calculation further predicts that the $A/{}^3\text{He}$ ratio at 3N-SRC region scales as $a_2(A)^2$ [25], giving a ${}^3\text{H}/{}^3\text{He}$ cross section ratio of $(a_2({}^3\text{H})/a_2({}^3\text{He}))^2 \approx 0.7$ [25].

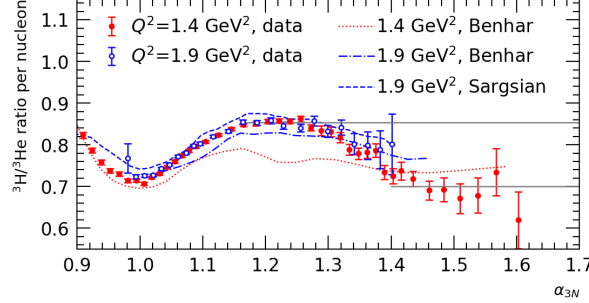


FIG. 3. ${}^3\text{H}/{}^3\text{He}$ ratios for the highest- Q^2 data sets. The solid lines shown for $\alpha_{3N} > 1.2$ and 1.4 indicate the fitted value $R = 0.854$ in the 2N-SRC plateau region [11], and the prediction for the 3N-SRC region, $R \approx 0.7$ [25] respectively. The curves are calculations from Benhar [38, 39] and Sargsian [6].

Figure 3 shows the ${}^3\text{H}/{}^3\text{He}$ cross section ratios vs α_{3N} from the two high- Q^2 data sets. Similar to α_{2N} , α_{3N} approximates the light cone momentum fraction in the three nucleon system [24] reducing the kinematic Q^2 dependence. Dotted and dashed curves represent spectral function-based calculations of inclusive cross section ratios from [38, 39] and [6]. The two $Q^2 = 1.9 \text{ GeV}^2$ calculations are in good qualitative agreement with the data near the QE peak and in 2N SRC region, although they differ by $\sim 10\%$. The 1.4 GeV^2 calculation [39] does not describe the observed scaling, as it indicates a much stronger Q^2 dependence than seen in the data.

The horizontal lines in Fig. 3 indicate the observed cross section ratio in the 2N-SRC regime [11] and the predicted ratio for the 3N-SRC regime [25]. The large- α_{3N} data are consistent with this prediction, although the model estimated 3N-SRC dominance for $\alpha_{3N} \geq 1.6$ [25]. This was chosen because it corresponds to $k_{min} = 600 \text{ MeV}$, where the dominant linear configuration has two spectator nucleons with momenta above 300 MeV , suppressing mean-field contributions. Previous $A/{}^3\text{He}$ measurements [8, 9, 21, 25] also suggest that 3N-SRCs may not be isolated at the kinematics of this study.

However, examining 3-body nuclei has the advantage that only 2N- and 3N-SRCs can contribute beyond the mean-field region. This allows us to evaluate the 3N-SRC impact on the ratios as the 2N-SRC contributions decrease and the 3N-SRCs become more important

with increasing α . Because we are studying the onset of 3N-SRCs, rather than trying to isolate a region where they dominate, the entire transition region is of interest. If the $Q^2=1.4$ and 1.9 GeV^2 kinematics were sufficient to isolate 3N-SRC contributions, the decrease in the ratio would suggest that 3N-SRCs are dominated by isospin-independent momentum structures (triangle configuration or linear configuration with all nucleons equally likely to have the highest momentum), consistent with the calculations of [25] as well as *ab initio* Variational Monte Carlo calculations [40]. If the scattering at the largest α values is still a combination of 2N-SRC and 3N-SRC contributions, the decrease of the ratio suggests that the contribution from 3N-SRCs must be 0.7 or lower, suggesting a slight enhancement of the doubly-occurring nucleon at the largest initial momenta.

While the conclusions above do not assume that we have isolated 3N-SRC configurations, there is an argument that these kinematics might be dominated by 3N-SRCs. As demonstrated above with 2N-SRCs, scaling violation is highly suppressed in $^3\text{H}/^3\text{He}$, yielding the onset of 2N-SRC plateaus at lower Q^2 and α . The calculation of Ref. [25] assumed 3N-SRCs dominated for k_{min} above 600 MeV ($\alpha_{3N} \approx 1.6$), yielding two $k \approx 300 \text{ MeV}$ spectators, large enough to strongly suppress mean-field contributions in all nuclei. For $A=3$, our data show that the 2N-SRC scaling starts by $\alpha_{2N}=1.2$, corresponding to $k_{min} = 200 \text{ MeV}$. This suggests that for light nuclei, it may be sufficient to have spectators with $k \geq 200 \text{ MeV}$, corresponding to $k_{min} = 400 \text{ MeV}$, or $\alpha_{3N} > 1.4$ for 3N-SRC dominance as indicated by the grey line in Fig. 3. Since our data set has only one Q^2 value covering this range, we cannot verify the signature of 3N-SRC dominance scaling in both α_{3N} and Q^2 . A precise test of scaling will require measuring the ratio at two Q^2 values with high-precision over the full α_{3N} range.

In conclusion, we presented new measurements of the inclusive cross section ratios in kinematics corresponding to scattering from high-momentum nucleons in SRCs over a range of Q^2 . We examined the behavior at lower Q^2 values where the x -scaling predicted by the SRC model has been observed to break down in previous $A/{}^2\text{H}$ ratio measurements, and found that the requirements of scaling for the ratio of heavy nuclei to ${}^2\text{H}$, $Q^2 > 1.4 \text{ GeV}^2$, is reduced to $Q^2 \gtrsim 1 \text{ GeV}^2$ for the ratios of ${}^3\text{H}$ and ${}^3\text{He}$ to ${}^2\text{H}$. We further observed that the scaling behavior in the 2N-SRC region is observed down to $Q^2=0.6 \text{ GeV}^2$ in the ${}^3\text{H}/{}^3\text{He}$ ratio. This can be understood due to the reduced mean-field momenta in $A=3$ nuclei, which allows clean isolation of the SRC contributions at lower x and Q^2 values, along with the

expectation that scaling violating effects such as FSIs and CM motion of the SRCs should have significant cancellation in the comparison of the mirror nuclei ${}^3\text{H}$ and ${}^3\text{He}$.

This also represented the first extraction of the ${}^3\text{H}/{}^3\text{He}$ ratio beyond the 2N-SRC region, allowing us to examine the behavior of the cross section ratio as we move into kinematics where 3N-SRC contributions are expected. While no scaling behavior at $x > 2$ (i.e. the 3N-SRC plateau) were observed in previous experiments hence no kinematic requirements for 3N-SRC scaling were identified, the decrease of the ${}^3\text{H}/{}^3\text{He}$ ratio beyond the 2N-SRC region suggests that the possible 3N-SRC contributions yield a ${}^3\text{H}/{}^3\text{He}$ ratio below 0.7. This significantly limits the probabilities of 3N-SRC configurations where the singly-occurring nucleon has the largest momentum, and is consistent with an isospin-symmetric distribution of the highest-momentum nucleons, or a somewhat larger contribution from the doubly-occurring nucleons. While the data for $\alpha_{3N} > 1.4$ are consistent with scaling predictions and yield a ratio of $R \approx 0.7$, consistent with calculations [25], this is seen only at one Q^2 value. A complete test of scaling will require ${}^3\text{H}/{}^3\text{He}$ inclusive ratio measurements with high precision for multiple Q^2 values.

ACKNOWLEDGMENTS

We acknowledge useful discussions with M. Sargsian, O. Benhar, and the contribution of the Jefferson Lab target group and technical staff for design and construction of the Tritium target and their support running this experiment. This work was supported in part by the Department of Energy's Office of Science, Office of Nuclear Physics, under contracts DE-AC02-05CH11231, DE-FG02-88ER40410, DE-SC0014168, DE-FG02-96ER40950, and DE-SC0014168, the National Science Foundation including grant NSF PHY-1714809, and DOE contract DE-AC05-06OR23177 under which JSA, LLC operates JLab. Z.H.Y. acknowledges the support from the National Science Foundation of China under contract 12275148. A.S. acknowledges the support from the Science Committee of Republic of Armenia under grant 21AG-1C085.

[1] L. Frankfurt and M. Strikman, Phys. Rept. **160**, 235 (1988).

- [2] J. Arrington, N. Fomin, and A. Schmidt, Annual Review of Nuclear and Particle Science **72**, 307 (2022).
- [3] M. M. Sargsian *et al.*, J. Phys. **G29**, R1 (2003).
- [4] N. Fomin, D. Higinbotham, M. Sargsian, and P. Solvignon, Ann. Rev. Nucl. Part. Sci. **67**, 129 (2017).
- [5] L. L. Frankfurt, M. I. Strikman, D. B. Day, and M. Sargsyan, Phys. Rev. C **48**, 2451 (1993).
- [6] M. M. Sargsian, Phys. Rev. C **89**, 034305 (2014).
- [7] J. Arrington *et al.*, Phys. Rev. Lett. **82**, 2056 (1999).
- [8] N. Fomin *et al.*, Phys. Rev. Lett. **108**, 092502 (2012).
- [9] Z. Ye *et al.*, Phys. Rev. C **97**, 065204 (2018).
- [10] B. Schmookler *et al.* (CLAS), Nature **566**, 354 (2019).
- [11] S. Li, R. Cruz-Torres, N. Santiesteban, Z. H. Ye, *et al.*, Nature **609**, 41 (2022).
- [12] K. S. Egiyan *et al.*, Phys. Rev. C **68**, 014313 (2003).
- [13] E. Piasetzky, M. Sargsian, L. Frankfurt, M. Strikman, and J. W. Watson, Phys. Rev. Lett. **97**, 162504 (2006).
- [14] R. Subedi *et al.*, Science **320**, 1476 (2008).
- [15] R. Shneor *et al.*, Phys. Rev. Lett. **99**, 072501 (2007).
- [16] I. Korover *et al.*, Phys. Rev. Lett. **113**, 022501 (2014).
- [17] M. Duer *et al.* (CLAS), Phys. Rev. Lett. **122**, 172502 (2019).
- [18] D. Nguyen *et al.* (Jefferson Lab Hall A), Phys. Rev. C **102**, 064004 (2020).
- [19] J. Arrington, D. Higinbotham, G. Rosner, and M. Sargsian, Prog. Part. Nucl. Phys. **67**, 898 (2012).
- [20] R. Weiss, A. W. Denniston, J. R. Pybus, O. Hen, E. Piasetzky, A. Schmidt, L. B. Weinstein, and N. Barnea, Phys. Rev. C **103**, L031301 (2021).
- [21] N. Fomin, J. Arrington, and S. Li, The European Physical Journal A **59**, 205 (2023).
- [22] K. S. Egiyan *et al.*, Phys. Rev. Lett. **96**, 082501 (2006).
- [23] D. W. Higinbotham and O. Hen, Phys. Rev. Lett. **114**, 169201 (2015), arXiv:1409.3069 [nucl-ex].
- [24] M. M. Sargsian, D. B. Day, L. L. Frankfurt, and M. I. Strikman, Phys. Rev. C **100**, 044320 (2019).
- [25] D. B. Day, L. L. Frankfurt, M. M. Sargsian, and M. I. Strikman, Phys. Rev. C **107**, 014319

- (2023).
- [26] S. N. Santiesteban *et al.*, Phys. Rev. Lett. **132**, 162501 (2024).
 - [27] J. Arrington, D. Day, D. W. Higinbotham, and P. Solvignon, “Precision measurement of the isospin dependence in the 2N and 3N short range correlation region,” Jefferson Lab Experiment Proposal E12-11-112 (2011).
 - [28] L. Weinstein, W. Boeglin, O. Chen, and F. Hauenstein, “Proton and Neutron Momentum Distributions in $A = 3$ Asymmetric Nuclei,” Jefferson Lab Experiment Proposal E12-14-011 (2014).
 - [29] R. Cruz-Torres *et al.* (Jefferson Lab Hall A Tritium), Phys. Lett. B **797**, 134890 (2019).
 - [30] R. Cruz-Torres *et al.* (Jefferson Lab Hall A Tritium), Phys. Rev. Lett. **124**, 212501 (2020).
 - [31] J. Arrington, R. Cruz-Torres, T. J. Hague, L. Kurbany, S. Li, D. Meekins, and N. Santiesteban, Eur. Phys. J. A **59**, 188 (2023), arXiv:2304.09998 [nucl-ex].
 - [32] The $Q^2=1.4$ GeV² data were taken in the Fall 2018 with a different tritium cell with an areal density of 84.8 mg/cm².
 - [33] S. N. Santiesteban *et al.*, Nucl. Instrum. Meth. A **940**, 351 (2019).
 - [34] S. Li, “Ph.D Thesis, University of New Hampshire,” (2020).
 - [35] S. Santiesteban, “Ph.D Thesis, University of New Hampshire,” (2020).
 - [36] J. Alcorn *et al.*, Nucl. Instrum. Meth. A **522**, 294 (2004).
 - [37] M. M. Sargsian, T. V. Abrahamyan, M. I. Strikman, and L. L. Frankfurt, Phys. Rev. C **71**, 044615 (2005).
 - [38] O. Benhar and V. R. Pandharipande, Phys. Rev. C **47**, 2218 (1993).
 - [39] O. Benhar, Phys. Rev. C **87**, 024606 (2013).
 - [40] R. Wiringa, R. Schiavilla, S. C. Pieper, and J. Carlson, Phys. Rev. C **89**, 024305 (2014).